Kinematic and kinetic parameters to identify water polo players' eggbeater kick techniques

Eisuke Kawai [a*], Tomohiro Gonjo [b], Hideki Takagi [c]

[a] *Faculty of Physical Education, International Budo University, Katsuura, Japan*

[b] *Department of Physical Performance, Norwegian School of Sport Sciences, Oslo, Norway*

[c] *Faculty of Health and Sport Sciences, University of Tsukuba, Tsukuba, Japan*

* corresponding author

841 Shinkan, Katsuura-City, Chiba-Prefecture, 299-5295, Japan

TEL: +81-470-73-4111

FAX: +81-470-73-4148

E-mail

Eisuke Kawai: e.kawai@budo-u.ac.jp

Tomohiro Gonjo: tomohiro.gonjo@nih.no

Hideki Takagi: takagi.hideki.ga@u.tsukuba.ac.jp

ORCID

Eisuke Kawai: https://orcid.org/0000-0003-1847-977X

Tomohiro Gonjo: http://orcid.org/0000-0001-9118-5167

Hideki Takagi: https://orcid.org/0000-0001-8797-7014

Keywords

aquatic sports; treading water; pressure distribution analysis; motion analysis; fluid force

Kinematic and kinetic parameters to identify water polo players' eggbeater kick techniques

This study aimed to clarify the kinematic and kinetic parameters that identify the technical differences in the eggbeater kick. Twelve water polo players performed the eggbeater kick, and its kinematics were recorded by a motion capture system. Pressure distributions around the feet were measured by sixteen pressure sensors attached to the dorsal and plantar surfaces of the feet, from which the resultant fluid force acting on the feet and the vertical component of the force (i.e., propulsive force) were estimated. Repeated-measures analysis of variance (including post hoc test) results showed that the pressure difference, due to negative pressure on the dorsal side of the foot, around the first toe was significantly larger than the other foot segments (difference of up to 7 kN/m^2, $P < 0.01$). Moreover, cluster analysis (including Fisher information) results showed that the kinetic (fluid force and pressure) data had a major influence on clustering; the highest Fisher information was 10.42 for the mean propulsive force. Among the kinematic foot parameters, the influence of the foot angle data on clustering was large, suggesting its importance as a technical parameter of the eggbeater kick in relation to the kinetic data.

Keywords: aquatic sports; treading water; pressure distribution analysis; motion analysis; fluid force

Introduction

Eggbeater kick is a treading water technique which is primarily used in water polo and artistic (synchronised) swimming. During eggbeater kicking, athletes continuously alternate circular movements of their lower-limbs to generate upward propulsive forces that elevate the body. The generation of propulsive forces by the eggbeater kick enables the water polo players to keep the upper body above the water during passing, shooting, blocking, and to resist an opponent's action during contact play (McCluskey et al., 2010; Nakashima, Minami & Takagi, 2015; Nakashima, Nakayama, Minami & Takagi, 2014;

Platanou, 2004; Smith, 1998). Therefore, performing an effective eggbeater kick is important for all water polo players.

Previous studies investigated the lower-limb kinematics of the eggbeater kick. It has been observed that high-level water polo players and artistic swimmers maintain the lateral distance between the left and right knees wide with the vertical displacement of the knee joints close to the water surface by abducting and flexing the hip joints (Homma & Homma, 2005; Oliveira, Chiu & Sanders, 2015). In addition, kinematic foot parameters, such as velocity, attack angle, sweepback angle, and paths of the feet, have been investigated due to their importance in generating propulsion upward during the eggbeater kick (Sanders, 1999a, 1999b). For effective propulsion (i.e., maintaining the upper body above water), the feet should maintain high speeds throughout the whole cycle with emphasising horizontal motions rather than vertical motions (Sanders, 1999a).

In recent years, kinetic parameters in the eggbeater kick have also been studied. Researchers have proposed a method for estimating the upward propulsive force using the inverse dynamics approach (Oliveira et al., 2015; Oliveira & Sanders, 2015; Oliveira, Saunders & Sanders, 2016). Moreover, in the latest studies, a method of estimating the propulsive force by pressure distribution analysis (PDA) has been applied to the eggbeater kick (Kawai, Tsunokawa, Sakaue & Takagi, 2020; Kawai, Tsunokawa & Takagi, 2018). The PDA method uses pressure sensors attached to body parts (such as feet and hands) and obtains time-series fluid force data generated by the parts of the body from measured pressure values. The pressure distribution around the part of the body reflects the influence of unsteady water flow, such as motion-generated vortices (Takagi, Nakashima, Ozaki & Matsuuchi, 2013; Takagi et al., 2014; T. Tsunokawa, Tsuno, Mankyu, Takagi & Ogita, 2018). In other words, the force information obtained by this method includes the effect of the water unsteadiness. The force data obtained in unsteady conditions yield results closer to reality than those in quasi-steady conditions (Kudo, Sakurai, Miwa & Matsuda, 2017; Tsunokawa, Mankyu, Takagi & Ogita, 2019; Tsunokawa et al., 2018). Kawai et al. (2018) conducted the incremental load test with weights to confirm the validity and reliability of the fluid force analysis during the eggbeater kick using the PDA method. As a result, a strong linear relation was found between the fluid force estimated by the PDA method and the net vertical load of the player (R^2 = 0.97 ± 0.02), and the reliability of the test-retest method was also high. Moreover, Kawai et al. (2020) conducted the PDA and three-dimensional (3D) motion analysis during the eggbeater kick with national-level water polo players and found that the increase in the propulsive force was mainly related to the decrease in pressure on the dorsal side of the foot and the propulsive force peaked when the foot reached its maximum velocity and began to decelerate.

In these previous studies, the eggbeater kick technique was often discussed through a comparison based on competition level (such as league ranking and years of experience), providing athletes and coaches with useful suggestions for improving performance. However, a high competition level might not necessarily guarantee a good eggbeater kick technique as some athletes might reach a top-level due to proficiency in other skills required in water polo games (such as swimming, throwing, wrestling and tactical actions). In other words, it is possible that previous eggbeater kick studies focusing on competitive levels might have overlooked key factors that determine the eggbeater kick technique. Therefore, as a first step, it is useful to investigate which parameters distinguish eggbeater kick techniques other than the competition level. If such parameters are identified in both kinematics and kinetics (hydrodynamics), they can serve as criteria for assessing good or bad eggbeater kicking technique (i.e., checkpoints for further performance improvement), especially in high-level players.

Therefore, we aimed to clarify the kinematic and kinetic parameters that identify technical differences in the eggbeater kick. We hypothesised that technical differences are likely to appear in the kinetic parameters (i.e., fluid force and pressure data).

Methods

Participants

Participants were twelve national-level male university water polo players (age 19.8 ± 0.9 years, height 1.77 ± 0.07 m, body mass 76.9 ± 9.4 kg, competitive experience 9.1 ± 2.6 years). At the time of this study, the participants had six sessions of water polo training per week. Each participant received an oral explanation of the potential risks and benefits of the study and gave written informed consent to participate. The study design and risks were reviewed and approved by the Research Ethics Committee of the university.

Experimental setup

Testing was performed in an experimental aquatic flume with underwater glass windows (Figure 1[A]). The participants performed maximal effort eggbeater kicks with no arm sculls, aiming to maintain the highest possible body position (Homma & Homma, 2005; Melchiorri et al., 2015; Oliveira et al., 2015). The participants were instructed to cross their arms in front of the chest and hold their breath during the trial. Their eggbeater kick motions were recorded using a motion capture system composed of twelve cameras (VENUS 3D, Nobby Tech. Ltd., Japan, sampling frequency 100 Hz). Two cameras were positioned in the flume, and ten cameras were located outside the flume with the cameras viewing the testing space through the windows (three front cameras, three back cameras, and four bottom cameras). Anatomical landmarks (left-right greater trochanters, superior anterior iliac spines, knee joints, ankle joints, first and fifth toes and heels; total eighteen points) were marked by wireless light-emitting diode markers (Kirameki, Nobby Tech. Ltd., Japan). To measure the pressure distribution around the feet, sixteen waterproof pressure sensors (PS-05KC, Kyowa Electronic Instruments Co. Ltd., Japan) were attached to the right and left foot (four each on the dorsal and plantar surfaces) (Kawai et al., 2020; Kawai et al., 2018). The data measured by the pressure sensors were recorded on a laptop computer with a sampling frequency of 100 Hz via a universal recorder (EDX-100A, Kyowa Electronic Instruments Co. Ltd., Japan). The measurements were performed for 5 s (Homma & Homma, 2005; Platanou, 2004). The motion and pressure data were synchronised by a dedicated synchroniser (eSync, Nobby Tech. Ltd., Japan).

[Figure 1 near here]

Definition of coordinate systems

The measurement area was calibrated by a dynamic calibration method, which resulted in the standard error of calibration of less than 0.0003 m. The global right-handed coordinate system (*X*-*Y*-*Z*) was defined by a dedicated base plate (*X*-axis: horizontal direction, *Y*-axis: longitudinal direction, *Z*-axis: vertical direction, downward was positive) (Figure 1[A]). The local right-handed coordinate systems (*x*-*y*-*z*) of the feet have their origin at the centre (*C*) of the plane formed by the first toe, fifth toe and heel of the right and left foot (Figure 1[B]). The *y*-axis was formed by a line connecting the heel and the local origin *C*, with the positive direction towards the toes; the *x*-axis was set perpendicular to the *y*-axis in the same horizontal plane (positive directions of the right and left foot corresponded to the fifth and first toe direction, respectively); and the *z*-axis was set perpendicular to both the *x*- and *y*-axes.

Kinematic foot parameters and motion structure of eggbeater kick

The 3D coordinates of the anatomical landmarks recorded by the motion capture system were filtered by a low-pass Butterworth digital filter with a 6 Hz cut-off frequency (Oliveira et al., 2015; Oliveira & Sanders, 2015; Oliveira et al., 2016). The kinematic foot parameters obtained in this study were attack and sweepback angles, as well as the resultant velocity and acceleration of *C* (Figure 1[B]). The attack angle was determined as the angle between the velocity vector of *C* and the plane of the foot (Kawai et al., 2020; Oliveira et al., 2015). The sweepback angle was determined as the angle between the projection of the velocity vector of *C* onto the plane of the foot and the *x*-axis of the foot local coordinate system (Sanders, 1999b). The right sweepback angle was defined as positive in a counter-clockwise direction, and the 0° (360°) was when the projected velocity vector and the *x*-axis overlapped in the foot plane. The left sweepback angle was defined to mirror the right sweepback angle. The motion ranges in each direction (*X*, *Y*, *Z* directions) were calculated as the difference between the maximum and minimum values of the 3D coordinates of *C*, normalised by its 3D movement path length.

One cycle of the eggbeater kick was determined as the period between two sequential maximally flexed positions of the right knee. The eggbeater kick is a two-phase motion; the out-kick (from maximal knee flexion to maximal knee extension) and the in-kick (from maximal knee extension to maximal knee flexion) with right and left leg motions being out of phase (Homma & Homma, 2005; Kawai et al., 2020). This means the right and left leg started one cycle from the out-kick and in-kick phase, respectively.

Estimation of fluid force (resultant force and propulsive force)

Fluid forces were calculated by a previously reported method (Kawai et al., 2020; Kawai et al., 2018). The foot was divided into four segments (segment 1–4: around the first toe, third toe, fifth toe and heel, respectively), and a pair of pressure sensors were attached to the dorsal and plantar side of each segment (Figure 1[A]). The measured pressure data were filtered by a low-pass Butterworth digital filter with a 10 Hz cut-off frequency (Kawai et al., 2020; Kudo, Matsuda, Sakurai, Ichikawa & Ikuta, 2018; Tsunokawa, Nakashima & Takagi, 2015). These measured data included dynamic pressures as well as static pressures due to the depths of sensors. Hence, each pressure sensor's depth was estimated from the foot coordinates (first toe, fifth toe and heel), and static pressures were subtracted from the total pressures so that the calculated pressures included only dynamic pressures (dorsal side, $P_{dorsal\_1–4}$; plantar side, $P_{plantar\_1–4}$). The fluid forces acting on each segment were estimated by

$$F_{segment\_i} = A_i \times P_{differ\_i} \qquad (1)$$

where $F_{segment\_i}$ (N) indicates the fluid force acting on the ith segment of the foot (for i of 1–4); A_i (m^2), the projected area of the ith segment; and P_{differ_i} (N/m^2), the plantar–dorsal pressure difference on the ith segment ($P_{plantar\_i} - Cos\ \theta_i\ P_{dorsal\_i}$). To calculate P_{differ_i}, we measured the angles between pairs of pressure sensors (θ_i) on the sagittal plane between the plantar and dorsal sides of the foot in the standing position and the obtained pressure differences were adjusted using θ_i. We then estimated the resultant fluid force acting on the entire foot (F_{foot} [N]) as

$$F_{foot} = \sum F_{segment\_i\ (i\ =\ 1–4)} \qquad (2)$$

Since the F_{foot} is considered to act perpendicularly to the plantar side of the foot, it was calculated from the vertical pressure on each segment of the foot on the plantar side. Accordingly, F_{foot} was directed parallel to the normal vector of the foot plane (calculated as the cross product of the heel–fifth toe and heel–first toe vectors). The vertical component of F_{foot} (F_z [N]) was calculated by multiplying F_{foot} by the Z

component of the unit normal vector of the foot plane. The fluid force acting on the *Z*-axis direction in the global coordinate system (F_z) was considered as the propulsive force produced during the eggbeater kick, which was defined as positive when acting towards the upward direction. The effectiveness of generated fluid force (i.e., propulsive efficiency) was calculated as the quotient of F_z and F_{foot}.

Statistical analysis

For statistical treatment of data, the assumption of normally distributed samples was verified with the Shapiro-Wilk test, and the sphericity assumption was confirmed by the Mauchly test. When the assumption of sphericity was not met, Greenhouse-Geisser's adjustment was used. The pressure data (i.e., P_{dorsal_i}, $P_{plantar\_i}$ and P_{differ_i}) were compared by one-way repeated-measures analysis of variance (ANOVA) with a paired t-test with Bonferroni correction (the segment as a within-participant factor) as a post hoc test. Cluster hierarchical analysis using the Ward's method was applied to classify eggbeater kicking groups within the participants, using all analysed variables (fluid force, pressure and foot kinematic data). Prior to the analyses, all variables were averaged over the right and left foot, and for the cluster analysis, all variables were standardised by

$$z = \frac{x - \bar{x}}{S} \quad (3)$$

where z is the standardised data, x is the original data, and $\bar{x}$ and S are the within-participant mean and standard deviation of the data, respectively. The valid number of clusters was selected using multiple methods, including the Calinski-Harabasz index, the elbow method, and the partition coefficient. In addition, the Fisher information was used to assess the influence of each variable on clustering (Figueiredo, Seifert, Vilas-Boas & Fernandes, 2012). The Fisher information corresponds to the ratio between inter-cluster and intra-cluster distances. The higher this value, the more discriminative are the variables, and < 1.0 shows a smaller inter-cluster than intra-cluster distance. The ANOVA test (including the post hoc test) and the cluster analysis were conducted with IBM SPSS statistics 26 (International Business Machines Corporation, NY, USA) at the $P < 0.05$ significance level, and the variables related to cluster validation were computed with MATLAB R2019 (The Mathworks, Inc., MA, USA).

Results

Averaged time series kinetic data (left-right F_{foot}, F_z, $P_{dorsal\_1–4}$ and $P_{plantar\_1–4}$) are shown in Figure 2[A] and [B]. Both left and right F_z peaked in the latter half of the out-kick phase. In foot segments 1, 2 and 4, P_{differ} increased due to the decrease in P_{dorsal} (i.e., the increase of negative pressure values). Main effects of the segments on P_{dorsal} (F = 54.433, $P < 0.001$), $P_{plantar}$ (F = 118.336, $P < 0.001$) and P_{differ} (F = 95.2, $P < 0.001$) were all significant. The negative pressure in segment 1 was significantly lower than the other segments, resulting in a large pressure difference (Figure 2[C]).

[Figure 2 near here]

The cluster analysis enabled us to classify the participants in four eggbeater kicking groups; two participants composed cluster #1, six participants were in cluster #2, two participants were categorised in cluster #3 and two participants composed cluster #4. The Fisher information was used to classify the variables from the most to the least discriminative variables. The Fisher information values for all variables were shown in Table 1. Overall, the fluid force and pressure data showed high Fisher information (i.e., major influence on clustering). For the kinematic foot parameters, angle data had more influence on clustering than velocity and acceleration data.

[Table 1 near here]

Discussion and implications

ANOVA (including post hoc test) results showed that the pressure difference, due to negative pressure on the dorsal side of the foot, around the first toe was significantly larger than the other foot segments (Figure 2[C]). Moreover, cluster analysis classified the participants into four eggbeater kick groups and demonstrated that the fluid force and pressure data had a major influence on clustering (Table 1). Among the kinematic foot parameters, the angular data showed a larger impact compared with foot velocity and acceleration.

In a previous study (Kawai et al., 2020), it was reported that the propulsive force during the eggbeater kick increased by the pressure difference between the plantar and dorsal side of the foot, which was mainly related to the decrease in pressure on the dorsal side. This phenomenon was similarly observed in both feet in this study (Figure 2[B]). The significant pressure difference in segment 1 (around the first toe) due to negative pressure on the dorsal side of the foot (Figure 2[C]) may be explained by the leading-edge vortex that is an essential factor in insect flight. These vortices are produced on the front side (leading part) of the wing and generate large negative pressures on the upper part of the wing (Ellington, Van Den Berg, Willmott & Thomas, 1996). Takagi et al. (2014) also observed a leading-edge vortex around the second finger on the dorsal side of a human swimmer’s hand and found that this vortex caused a large decrease in dorsal side pressure during the in-scull phase of sculling. With the exception of the beginning of the kick and recovery, the leading part of the foot during the eggbeater kick is the first toe side, which supports the possibility of lower negative pressure around the first toe produced by the leading-edge vortex. On the other hand, segment 3 (around the fifth toe) is far from the leading part, suggesting that the effect of the generated vortex is small. This might explain why the pressure difference between the plantar and dorsal side of this part of the foot was hardly observed, and consequently, the contribution to propulsion was also small. In fact, in hand sculling, the pressure difference around the fifth finger is also very small during the in-scull phase (Takagi et al., 2014). For effective propulsion during eggbeater kicking, water flow should be directed from the first toe side during the out-kick and the first half of the in-kick, for which the hip (flexion, abduction, internal rotation) and ankle (supination/pronation) movements are important (Homma & Homma, 2005; Oliveira et al., 2015). In addition, the negative propulsive force during the second half of the in-kick (recovery motion) should be minimised (Figure 2[A]).

Generating greater propulsive force on average throughout the cycle is an important point in eggbeater kick (Oliveira et al., 2015; Oliveira & Sanders, 2015; Oliveira et al., 2016), which is supported by the highest Fisher information (10.42) of the propulsive force observed in this study (Table 1). In the clustering of this study, cluster #1 and #3 showed better propulsive force exertion than the other two clusters. Among the variables with Fisher information greater than 1.0, these clusters showed similarly good results in terms of resultant fluid force, plantar side pressures in segment 1, 2 and 4 (around the first toe, third toe and heel) and maximum attack angle (Table 1). On the other hand, both velocity and acceleration results had Fisher information smaller than 1.0, meaning that even though velocity and acceleration are also known to be essential factors in propulsion, they might be less important than the attack angle in eggbeater kicking.

In wind-tunnel experiment using a hand model (under steady conditions), it has been reported that an attack angle of about 40° maximises the propulsive lift component (Schleihauf, 1979). Moreover, in a previous study investigating the hand sculling of world-class artistic swimmers using the PDA method (i.e., under unsteady conditions), the peak propulsive force (27.47 ± 7.25 N) was observed when the attack angle was about 20-50° (Homma, Okamoto & Takagi, 2019). The attack angle during sculling affects the pressure fluctuation around the hand (especially the leading part) and the resulting pressure difference induces the generation of unsteady fluid force (including propulsive force) (Homma, Kawai & Takagi, 2016; Takagi et al., 2014). In front crawl swimming, Koga et al. (2020) also reported that the propulsive force decreased as the attack angle decreased even when the hand velocity increased. Our results and evidence in other aquatic motion from the literature suggest that foot angle data may be the most important kinematic factor to generate large hydrodynamic forces. Interestingly, even though the negative pressure on the dorsal side of the foot plays a major role in producing propulsion in the eggbeater kick, the cluster analysis detected larger Fisher information in pressure results on the plantar than the dorsal side. This might mean that technical differences (e.g., attack angle differences) may be linked to the positive pressure on the plantar side, which should be investigated in the future.

In this study, the PDA method was applied to both feet for the first time to estimate the propulsive force during the eggbeater kick. The PDA method can reveal detailed propulsion dynamics of the feet in unsteady conditions but cannot instead estimate the total propulsive force (i.e., propulsive force of the entire lower body) of the eggbeater kick. In the future, the combination of the PDA method and the inverse dynamics approach (Oliveira et al., 2015; Oliveira & Sanders, 2015; Oliveira et al., 2016), which allows the estimation of the total propulsive force, may provide an estimate of the contribution to propulsion in other body parts, such as the lower leg. Moreover, even though the high Fisher information of the hydrodynamic data in this study is a fairly reasonable result, further study is required with larger sample sizes to consolidate these findings. In addition, it should be recognised that the use of more game-specific technique (i.e., eggbeater kick with hand sculling) might yield different results, which should also be investigated in future studies.

Conclusion

It is likely that hydrodynamic and foot angle parameters are important factors to characterise eggbeater kick techniques and are useful to evaluate the eggbeater kick technique of water polo players (especially in high competition level) in the future.

Acknowledgements

We are grateful to all members of the Swimming Laboratory at the University of Tsukuba for their helpful advice. In addition, we thank all players for their participation in this study.

Funding details

This work was supported by Japan Society for the Promotion of Science (JSPS) KAKENHI Grant Number JP19K24290.

Disclosure statement

No potential conflict of interest was reported by the authors.

References

Ellington, C. P., Van Den Berg, C., Willmott, A. P. & Thomas, A. L. (1996). Leading-edge vortices in insect flight. *Nature, 384*(6610), 626–630.

Figueiredo, P., Seifert, L., Vilas-Boas, J. P. & Fernandes, R. J. (2012). Individual profiles of spatio-temporal coordination in high intensity swimming. *Human Movement Science, 31*(5), 1200–1212. doi:10.1016/j.humov.2012.01.006

Homma, M. & Homma, M. (2005). Coaching points for the technique of the eggbeater kick in synchronised swimming based on three-dimensional motion analysis. *Sports Biomechanics, 4*(1), 73–87. doi:10.1080/14763140508522853

Homma, M., Kawai, Y. & Takagi, H. (2016). Estimating hydrodynamic forces acting on the hand during sculling in synchronised swimming. In M. Ae, Y. Enomoto, N. Fujii & H. Takagi (Eds.), *34th International Conference on Biomechanics in Sports* (pp. 656–659). Tsukuba.

Homma, M., Okamoto, Y. & Takagi, H. (2019). How do elite artistic swimmers generate fluid forces by hand during sculling motions? *Sports Biomechanics*, 1–15. doi:10.1080/14763141.2019.1671485

Kawai, E., Tsunokawa, T., Sakaue, H. & Takagi, H. (2020). Propulsive forces on water polo players' feet from eggbeater kicking estimated by pressure distribution analysis. *Sports Biomechanics*, 1–15. doi:10.1080/14763141.2020.1797152

Kawai, E., Tsunokawa, T. & Takagi, H. (2018). Estimating the hydrodynamic forces during eggbeater kicking by pressure distribution analysis. *Heliyon*, *4*(12), e01095. doi:10.1016/j.heliyon.2018.e01095

Koga, D., Gonjo, T., Kawai, E., Tsunokawa, T., Sakai, S., Sengoku, Y., Homma, M. & Takagi, H. (2020). Effects of exceeding stroke frequency of maximal effort on hand kinematics and hand propulsive force in front crawl. *Sports Biomechanics*, 1–13. doi: 10.1080/14763141.2020.1814852

Kudo, S., Matsuda, Y., Sakurai, Y., Ichikawa, H. & Ikuta, Y. (2018). Relationship between the angular velocity of the shoulder joint and hand propulsion in front crawl stroke. In H. Takagi, Y. Ohgi, Y. Sengoku & T. Gonjo (Eds.), *XIII th International Symposium on Biomechanics and Medicine in Swimming Proceedings* (pp. 79–83). Tokyo: Impress R&D.

Kudo, S., Sakurai, Y., Miwa, T. & Matsuda, Y. (2017). Relationship between shoulder roll and hand propulsion in the front crawl stroke. *Journal of Sports Sciences*, *35*(10), 945–952. doi:10.1080/02640414.2016.1206208

McCluskey, L., Lynskey, S., Leung, C. K., Woodhouse, D., Briffa, K. & Hopper, D. (2010). Throwing velocity and jump height in female water polo players: performance predictors. *Journal of Science and Medicine in Sport*, *13*(2), 236–240. doi:10.1016/j.jsams.2009.02.008

Melchiorri, G., Viero, V., Triossi, T., Tancredi, V., Galvani, C. & Bonifazi, M. (2015). Testing and training of the eggbeater kick movement in water polo: applicability of a new method. *Journal of Strength and Conditioning Research*, *29*(10), 2758–2764. doi:10.1519/JSC.0000000000000946

Nakashima, M., Minami, Y. & Takagi, H. (2015). Optimising simulation for lower limb motion during throwing in water polo. *Mechanical Engineering Journal*, *2*(4), 14-00472. doi:10.1299/mej.14-00472

Nakashima, M., Nakayama, Y., Minami, Y. & Takagi, H. (2014). Development of the simulation model for throwing motion in water polo. *Sports Engineering, 17*(1), 45–53. doi:10.1007/s12283-013-0127-x

Oliveira, N., Chiu, C. Y. & Sanders, R. H. (2015). Kinematic patterns associated with the vertical force produced during the eggbeater kick. *Journal of Sports Sciences, 33*(16), 1675–1681. doi:10.1080/02640414.2014.1003590

Oliveira, N. & Sanders, R. H. (2015). Kinematic and kinetic evidence for functional lateralization in a symmetrical motor task: the water polo eggbeater kick. *Experimental Brain Research, 233*(3), 947–957. doi:10.1007/s00221-014-4166-8

Oliveira, N., Saunders, D. H. & Sanders, R. H. (2016). The effect of fatigue-induced changes in eggbeater-kick kinematics on performance and risk of injury. *International Journal of Sports Physiology and Performance, 11*(1), 141–145. doi:10.1123/ijspp.2015-0057

Platanou, T. (2004). Time-motion analysis of international level water polo players. *Journal of Human Movement Studies, 46*, 319–331.

Sanders, R. H. (1999a). Analysis of the eggbeater kick used to maintain height in water polo. *Journal of Applied Biomechanics, 15*(3), 284–291. doi:10.1123/jab.15.3.284

Sanders, R. H. (1999b). A model of kinematic variables determining height achieved in water polo boosts. *Journal of Applied Biomechanics, 15*(3), 270–283. doi:10.1123/jab.15.3.270

Schleihauf, R. (1979). A hydrodynamic analysis of swimming propulsion. In J. Terauds & E.W. Bedingfield (Eds.), *Swimming III* (pp. 173–184). Baltimore, MD: University Park Press.

Smith, H. K. (1998). Applied physiology of water polo. *Sports Medicine, 26*(5), 317–334. doi:10.2165/00007256-199826050-00003

Takagi, H., Nakashima, M., Ozaki, T. & Matsuuchi, K. (2013). Unsteady hydrodynamic forces acting on a robotic hand and its flow field. *Journal of Biomechanics, 46*(11), 1825–1832. doi:10.1016/j.jbiomech.2013.05.006

Takagi, H., Shimada, S., Miwa, T., Kudo, S., Sanders, R. & Matsuuchi, K. (2014). Unsteady hydrodynamic forces acting on a hand and its flow field during sculling motion. *Human Movement Science, 38*, 133–142. doi:10.1016/j.humov.2014.09.003

Tsunokawa, T., Mankyu, H., Takagi, H. & Ogita, F. (2019). The effect of using paddles on hand propulsive forces and froude efficiency in arm-stroke-only front-crawl swimming at various velocities. *Human Movement Science, 64*, 378–388. doi:10.1016/j.humov.2019.03.007

Tsunokawa, T., Nakashima, M. & Takagi, H. (2015). Use of pressure distribution analysis to estimate fluid forces around a foot during breaststroke kicking. *Sports Engineering, 18*(3), 149–156. doi:10.1007/s12283-015-0174-6

Tsunokawa, T., Tsuno, T., Mankyu, H., Takagi, H. & Ogita, F. (2018). The effect of paddles on pressure and force generation at the hand during front crawl. *Human Movement Science, 57*, 409–416. doi:10.1016/j.humov.2017.10.002

Table 1. Mean value of each cluster for all variables. Fisher information represents the influence of each variable on the clustering.

Figure 1. (A) Schematic representation of the experiment. The testing was performed in an experimental aquatic flume. The participants' eggbeater kicking motions were recorded by a motion capture system composed of twelve cameras. The pressure distributions around the feet were measured by sixteen waterproof pressure sensors attached to the dorsal and plantar surfaces of the participants' both feet. (B) Local right-handed coordinate systems of the feet and kinematic foot parameters.

Figure 2. (A) Resultant force (F_{foot}) and propulsive force (F_z) fluctuations during one eggbeater kick cycle (averaged over n = 12). Stick graphics represent eggbeater kicking motion viewed from the frontal plane. Black and grey bars indicate the motion-phases (out- and in-kick) of the right and left foot, respectively. (B) Dynamic pressure (dorsal side, P_{dorsal_i}; plantar side, $P_{plantar\_i}$) fluctuations of each segment during one eggbeater kick cycle (averaged over n = 12). Black and grey vertical dotted lines indicate the F_z peaks for the right and left foot, respectively. (C) Differences in pressure data between the foot segments (top, P_{dorsal_i}; centre, $P_{plantar\_i}$; bottom, pressure difference P_{differ_i}). ***** and ****** show significant differences at $P < 0.05$ and $P < 0.01$, respectively.

Table 1

Variables	Unit	Cluster				Fisher information
		1 (n = 2)	2 (n =6)	3 (n =2)	4 (n =2)	
Normalised F_z (ave)	N/kg	1.10	0.77	1.23	0.97	10.42
Normalised F_{foot} (ave)	N/kg	1.52	1.11	1.70	1.39	9.65
$P_{plantar\_1}$ (ave)	kN/m^2	0.66	−0.45	1.23	0.06	5.98
Normalised F_{foot} (max)	N/kg	3.97	2.87	4.41	3.36	4.88
$P_{plantar\_4}$ (ave)	kN/m^2	0.92	−1.00	0.71	−0.81	4.57
Normalised F_z (min)	N/kg	−0.07	−0.14	0.05	−0.15	4.41
Normalised F_z (max)	N/kg	2.93	2.30	3.34	3.04	3.10
$P_{plantar\_2}$ (ave)	kN/m^2	1.08	0.22	1.83	0.25	2.54
P_{dorsal_4} (ave)	kN/m^2	−4.10	−4.04	−3.58	−4.88	2.34
Normalised F_{foot} (min)	N/kg	−0.17	−0.32	0.07	−0.28	1.78
P_{dorsal_1} (ave)	kN/m^2	−5.73	−5.70	−6.29	−7.67	1.66
$P_{plantar\_3}$ (ave)	kN/m^2	−2.41	−4.10	−1.89	−4.76	1.58
P_{dorsal_2} (ave)	kN/m^2	−3.43	−3.72	−3.21	−4.82	1.48
Attack angle (max)	°	35.7	28.4	38.3	29.0	1.36
Attack angle (min)	°	−24.4	−8.3	−15.0	−10.4	1.21
Corrected sweepback angle in out-kick phase (ave)	°	478.9	479.3	471.5	481.7	0.84
Kick velocity (ave)	m/s	2.73	2.71	2.77	2.92	0.82
P_{dorsal_3} (ave)	kN/m^2	−2.95	−2.89	−2.12	−2.93	0.72
Kick acceleration (ave)	m/s^2	−0.42	−0.09	−0.32	0.05	0.69
Normalised vertical motion range	%	35.2	32.1	32.1	29.9	0.66
Kick velocity (min)	m/s	1.35	1.48	1.57	1.75	0.61
Kick velocity (max)	m/s	3.80	3.81	3.79	3.97	0.51
Normalised longitudinal motion range	%	20.4	23.5	24.7	24.5	0.43
Attack angle (ave)	°	11.6	10.2	12.7	9.6	0.24
Propulsive efficiency	%	72.8	68.9	72.2	69.6	0.24
Kick acceleration (min)	m/s^2	−29.3	−25.6	−26.6	−27.3	0.17
Normalised horizontal motion range	%	23.4	22.7	20.7	22.8	0.14
Kick acceleration (max)	m/s^2	34.5	32.5	30.9	33.3	0.05

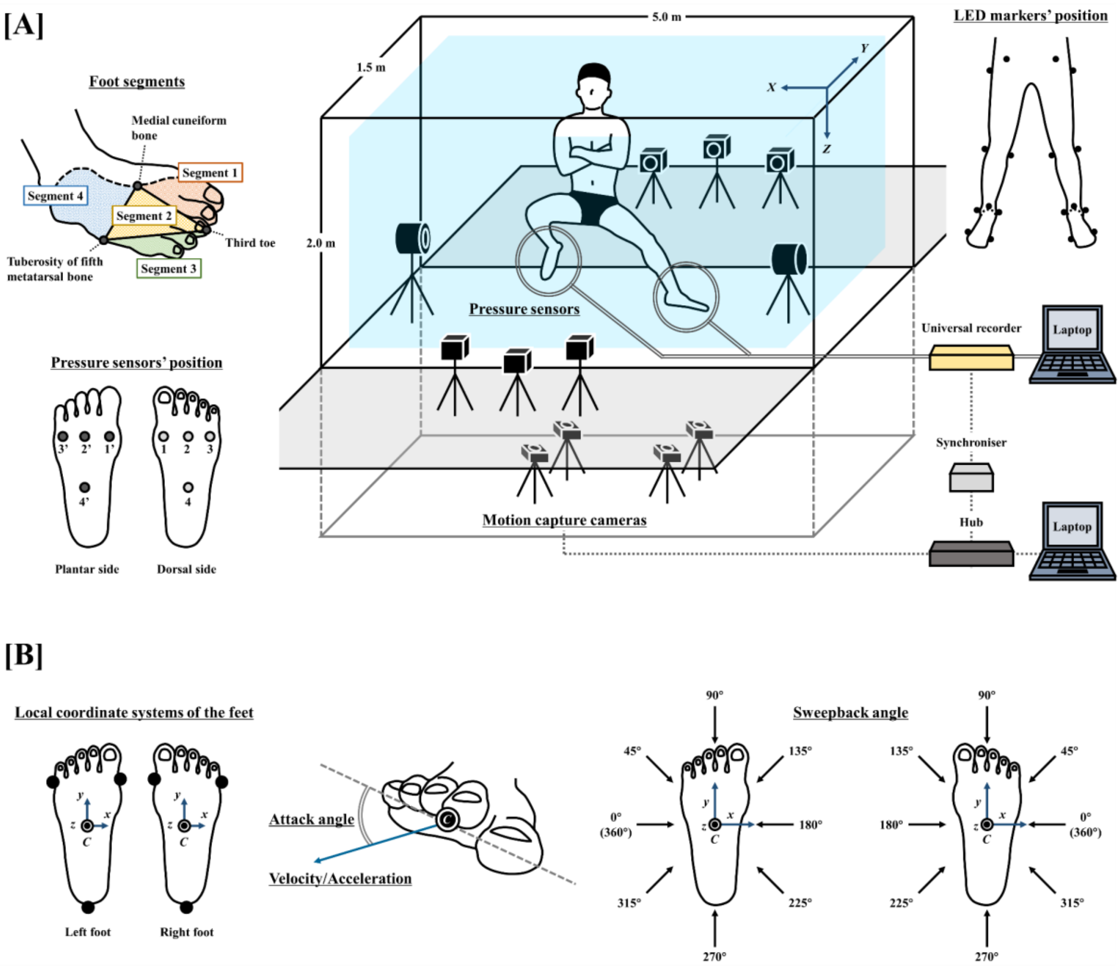
[A]
Foot segments
Medial cuneiform bone
Segment 1
Segment 4
Segment 2
Third toe
Tuberosity of fifth metatarsal bone
Segment 3
Pressure sensors' position
3' 2' 1'
4'
1 2 3
4
Plantar side
Dorsal side
5.0 m
1.5 m
2.0 m
Y
X
Z
Pressure sensors
Motion capture cameras
LED markers' position
Universal recorder
Laptop
Synchroniser
Hub
Laptop
[B]
Local coordinate systems of the feet
Left foot
Right foot
Attack angle
Velocity/Acceleration
Sweepback angle
90°
45°
135°
0° (360°)
180°
315°
225°
270°

Figure 1

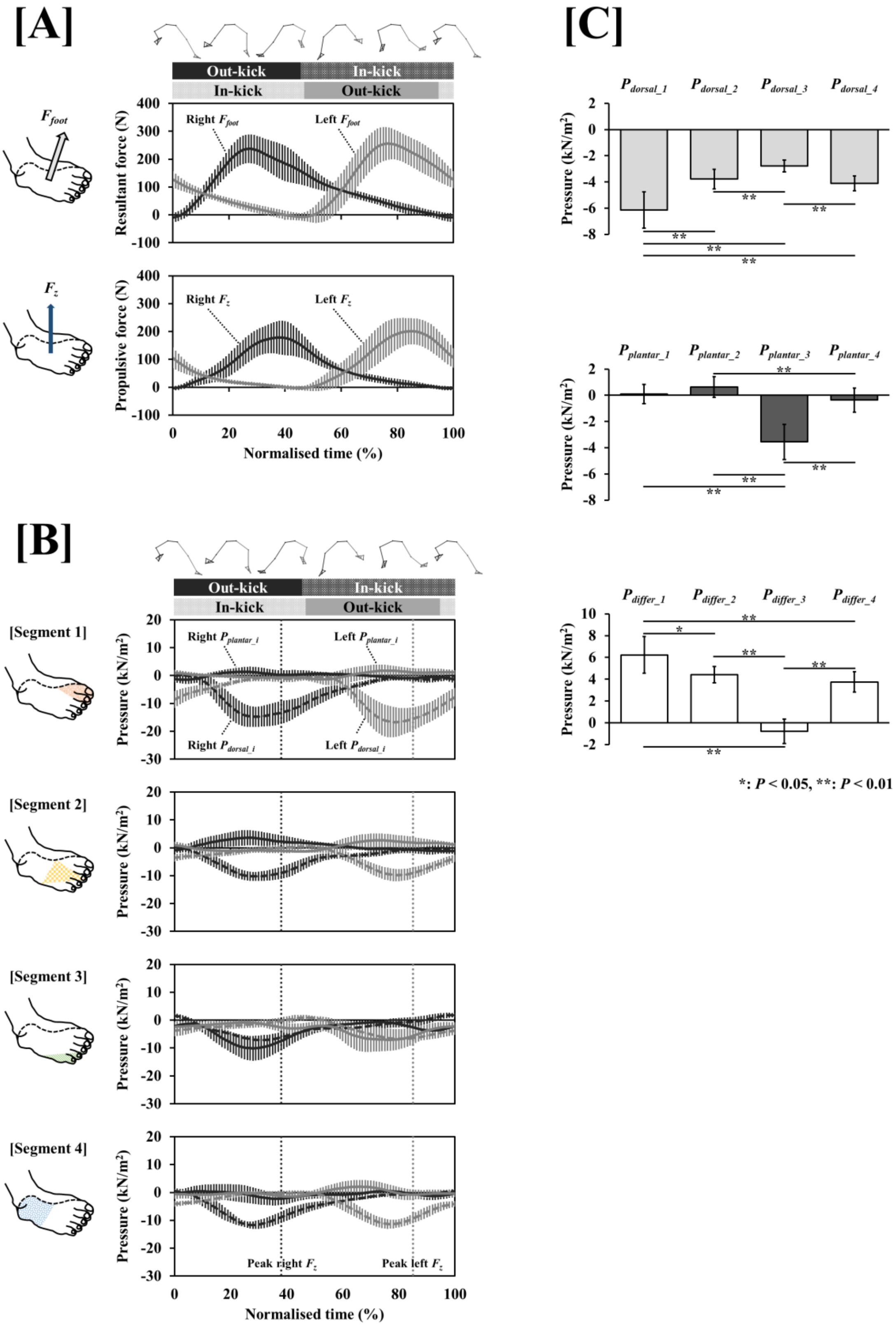
[A]
Out-kick
In-kick
In-kick
Out-kick
F_{foot}
Resultant force (N)
Right F_{foot}
Left F_{foot}
F_z
Propulsive force (N)
Right F_z
Left F_z
Normalised time (%)
[B]
[Segment 1]
[Segment 2]
[Segment 3]
[Segment 4]
Pressure (kN/m²)
Right $P_{plantar\_i}$
Left $P_{plantar\_i}$
Right P_{dorsal_i}
Left P_{dorsal_i}
Peak right F_z
Peak left F_z
Normalised time (%)
[C]
P_{dorsal_1} P_{dorsal_2} P_{dorsal_3} P_{dorsal_4}
$P_{plantar\_1}$ $P_{plantar\_2}$ $P_{plantar\_3}$ $P_{plantar\_4}$
P_{differ_1} P_{differ_2} P_{differ_3} P_{differ_4}
Pressure (kN/m²)
*: $P < 0.05$, **: $P < 0.01$

Figure 2